

# RADIATIVE TRANSFER IN THE OCEAN

C. D. Mobley, Sequoia Scientific, Inc., WA, USA

Copyright © 2001 Academic Press

doi:10.1006/rwos.2001.0469

## Introduction

Understanding how light interacts with sea water is a fascinating problem in itself, as well as being fundamental to fields as diverse as biological primary production, mixed-layer thermodynamics, photochemistry, lidar bathymetry, ocean-color remote sensing, and visual searching for submerged objects. For these reasons, optics is one of the fastest growing oceanographic research areas.

Radiative transfer theory provides the theoretical framework for understanding light propagation in the ocean, just as hydrodynamics provides the framework for physical oceanography. The article begins with an overview of the definitions and terminology of radiative transfer as used in oceanography. Various ways of quantifying the optical properties of a water body and the light within the water are described. The chapter closes with examples of the absorption and scattering properties of two hypothetical water bodies, which are characteristic of the open ocean and a turbid estuary, and a comparison of their underwater light fields.

## Terminology

The optical properties of sea water are sometimes grouped into inherent and apparent properties.

- Inherent optical properties (IOPs) are those properties that depend only upon the medium and therefore are independent of the ambient light field. The two fundamental IOPs are the absorption coefficient and the volume scattering function. (These quantities are defined below.)
- Apparent optical properties (AOPs) are those properties that depend both on the medium (the IOPs) and on the directional structure of the ambient light field, and that display enough regular features and stability to be useful descriptors of a water body. Commonly used AOPs are the irradiance reflectance, the remote-sensing reflectance, and various diffuse attenuation functions.

'Case 1 waters' are those in which the contribution by phytoplankton to the total absorption and scattering is high compared to that by other

substances. Absorption by chlorophyll and related pigments therefore plays the dominant role in determining the total absorption in such waters, although covarying detritus and dissolved organic matter derived from the phytoplankton also contribute to absorption and scattering in case 1 waters. Case 1 water can range from very clear (oligotrophic) to very productive (eutrophic) water, depending on the phytoplankton concentration.

'Case 2 waters' are 'everything else,' namely, waters where inorganic particles or dissolved organic matter from land drainage contribute significantly to the IOPs, so that absorption by pigments is relatively less important in determining the total absorption. Roughly 98% of the world's open ocean and coastal waters fall into the case 1 category, but near-shore and estuarine case 2 waters are disproportionately important to human interests such as recreation, fisheries, and military operations.

**Table 1** summarizes the terms, units, and symbols for various quantities frequently used in optical oceanography.

## Radiometric Quantities

Consider an amount  $\Delta Q$  of radiant energy incident in a time interval  $\Delta t$  centered on time  $t$ , onto a surface of area  $\Delta A$  located at position  $(x, y, z)$ , and arriving through a set of directions contained in a solid angle  $\Delta\Omega$  about the direction  $(\theta, \varphi)$  normal to the area  $\Delta A$ , as produced by photons in a wavelength interval  $\Delta\lambda$  centered on wavelength  $\lambda$ . The geometry of this situation is illustrated in **Figure 1**. Then an operational definition of the spectral radiance is

$$L(x, y, z, t, \theta, \varphi, \lambda) \equiv \frac{\Delta Q}{\Delta t \Delta A \Delta\Omega \Delta\lambda} \quad [1]$$

$[\text{J s}^{-1} \text{m}^{-2} \text{sr}^{-1} \text{nm}^{-1}]$

In the conceptual limit of infinitesimal parameter intervals, the spectral radiance is defined as

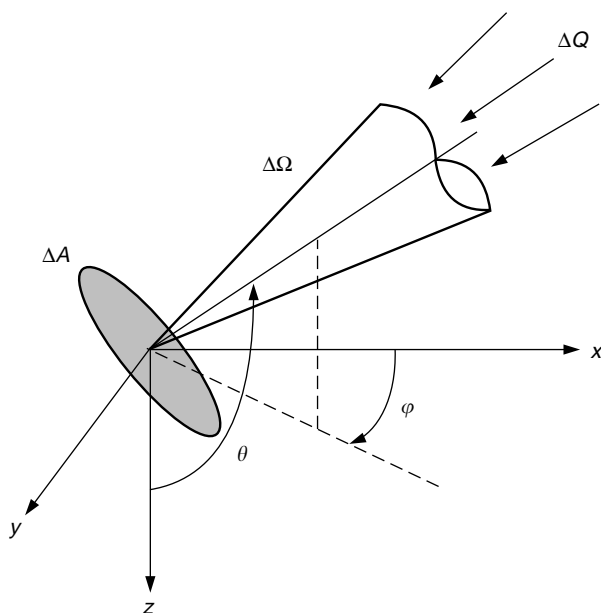
$$L(x, y, z, t, \theta, \varphi, \lambda) \equiv \frac{\partial^4 Q}{\partial t \partial A \partial\Omega \partial\lambda} \quad [2]$$

Spectral radiance is the fundamental radiometric quantity of interest in optical oceanography: it completely specifies the positional  $(x, y, z)$ , temporal  $(t)$ ,

**Table 1** Quantities commonly used in optical oceanography

Quantity	SI units	Symbol
<b>Radiometric quantities</b>		
Quantity of radiant energy	$\text{J nm}^{-1}$	$Q$
Power	$\text{W nm}^{-1}$	$\Phi$
Intensity	$\text{W sr}^{-1} \text{nm}^{-1}$	$I$
Radiance	$\text{W m}^{-2} \text{sr}^{-1} \text{nm}^{-1}$	$L$
Downwelling plane irradiance	$\text{W m}^{-2} \text{nm}^{-1}$	$E_d$
Upwelling plane irradiance	$\text{W m}^{-2} \text{nm}^{-1}$	$E_u$
Net irradiance	$\text{W m}^{-2} \text{nm}^{-1}$	$E$
Scalar irradiance	$\text{W m}^{-2} \text{nm}^{-1}$	$E_o$
Downwelling scalar irradiance	$\text{W m}^{-2} \text{nm}^{-1}$	$E_{o,d}$
Upwelling scalar irradiance	$\text{W m}^{-2} \text{nm}^{-1}$	$E_{o,u}$
Photosynthetic available radiation	$\text{Photons s}^{-1} \text{m}^{-2}$	PAR
<b>Inherent optical properties</b>		
Absorption coefficient	$\text{m}^{-1}$	$a$
Volume scattering function	$\text{m}^{-1} \text{sr}^{-1}$	$\beta$
Scattering phase function	$\text{sr}^{-1}$	$\bar{\beta}$
Scattering coefficient	$\text{m}^{-1}$	$b$
Backscatter coefficient	$\text{m}^{-1}$	$b_b$
Beam attenuation coefficient	$\text{m}^{-1}$	$c$
Single-scattering albedo	—	$\omega_o$
<b>Apparent optical properties</b>		
Irradiance reflectance (ratio)	—	$R$
Remote-sensing reflectance	$\text{sr}^{-1}$	$R_{rs}$
Attenuation coefficients	$\text{m}^{-1}$	
of radiance $L(z, \theta, \varphi)$	$\text{m}^{-1}$	$K(\theta, \varphi)$
of downwelling irradiance $E_d(z)$	$\text{m}^{-1}$	$K_d$
of upwelling irradiance $E_u(z)$	$\text{m}^{-1}$	$K_u$
of PAR	$\text{m}^{-1}$	$K_{PAR}$

directional  $(\theta, \varphi)$ , and spectral  $(\lambda)$  structure of the light field. In many oceanic environments, horizontal variations (on a scale of tens to thousands of meters) of the IOPs and the radiance are much less

**Figure 1** Geometry used to define radiance.

than variations with depth, in which case it can be assumed that these quantities vary only with depth  $z$ . (An exception would be the light field due to a single light source imbedded in the ocean; such a radiance distribution is inherently three-dimensional.) Moreover, since the timescales for changes in IOPs or in the environment (seconds to seasons) are much greater than the time required for the radiance to reach steady state (microseconds) after a change in IOPs or boundary conditions, time-independent radiative transfer theory is adequate for most oceanographic studies. (An exception is time-of-flight lidar bathymetry.) When the assumptions of horizontal homogeneity and time independence are valid, the spectral radiance can be written as  $L(z, \theta, \varphi, \lambda)$ .

Although the spectral radiance completely specifies the light field, it is seldom measured in all directions, both because of instrumental difficulties and because such complete information often is not needed. The most commonly measured radiometric quantities are various irradiances. Suppose the light detector is equally sensitive to photons of a given wavelength  $\lambda$  traveling in any direction  $(\theta, \varphi)$  within a hemisphere of directions. If the detector is located at depth  $z$  and is oriented facing upward, so as to

collect photons traveling downward, then the detector output is a measure of the spectral downwelling scalar irradiance at depth  $z$ ,  $E_{od}(z, \lambda)$ . Such an instrument is summing radiance over all the directions (elements of solid angle) in the downward hemisphere; thus  $E_{od}(z, \lambda)$  is related to  $L(z, \theta, \varphi, \lambda)$  by

$$E_{od}(z, \lambda) = \int_{2\pi_d} L(z, \theta, \varphi, \lambda) d\Omega \quad [\text{W m}^{-2} \text{nm}^{-1}] \quad [3]$$

Here  $2\pi_d$  denotes the hemisphere of downward directions (i.e., the set of directions  $(\theta, \varphi)$  such that  $0 \leq \theta \leq \pi/2$  and  $0 \leq \varphi < 2\pi$ , if  $\theta$  is measured from the  $+z$  or nadir direction). The integral over  $2\pi_d$  can be evaluated as a double integral over  $\theta$  and  $\varphi$  after a specific coordinate system is chosen.

If the same instrument is oriented facing downward, so as to detect photons traveling upward, then the quantity measured is the spectral upwelling scalar irradiance  $E_{ou}(z, \lambda)$ . The spectral scalar irradiance  $E_o(z, \lambda)$  is the sum of the downwelling and upwelling components:

$$\begin{aligned} E_o(z, \lambda) &\equiv E_{od}(z, \lambda) + E_{ou}(z, \lambda) \\ &= \int_{4\pi} L(z, \theta, \varphi, \lambda) d\Omega \end{aligned} \quad [4]$$

$E_o(z, \lambda)$  is proportional to the spectral radiant energy density ( $\text{J m}^{-3} \text{nm}^{-1}$ ) and therefore quantifies how much radiant energy is available for photosynthesis or heating the water.

Now consider a detector designed so that its sensitivity is proportional to  $|\cos \theta|$ , where  $\theta$  is the angle between the photon direction and the normal to the surface of the detector. This is the ideal response of a ‘flat plate’ collector of area  $\Delta A$ , which when viewed at an angle  $\theta$  to its normal appears to have an area of  $\Delta A |\cos \theta|$ . If such a detector is located at depth  $z$  and is oriented facing upward, so as to detect photons traveling downward, then its output is proportional to the spectral downwelling plane irradiance  $E_d(z, \lambda)$ . This instrument is summing the downwelling radiance weighted by the cosine of the photon direction, thus

$$\begin{aligned} E_d(z, \lambda) &= \int_{2\pi_d} L(z, \theta, \varphi, \lambda) |\cos \theta| d\Omega \\ &[\text{W m}^{-2} \text{nm}^{-1}] \end{aligned} \quad [5]$$

Turning this instrument upside down gives the spectral upwelling plane irradiance  $E_u(z, \lambda)$ .  $E_d$  and  $E_u$  are useful because they give the energy flux (power per unit area) across the horizontal surface

at depth  $z$  owing to downwelling and upwelling photons, respectively. The difference  $E_d - E_u$  is called the net (or vector) irradiance.

Photosynthesis is a quantum phenomenon, i.e., it is the number of available photons rather than the amount of radiant energy that is relevant to the chemical transformations. This is because a photon of, say,  $\lambda = 400 \text{ nm}$ , if absorbed by a chlorophyll molecule, induces the same chemical change as does a photon of  $\lambda = 600 \text{ nm}$ , even though the 400 nm photon has 50% more energy than the 600 nm photon. Only a part of the photon energy goes into photosynthesis; the excess is converted to heat or is re-radiated. Moreover, chlorophyll is equally able to absorb and utilize a photon regardless of the photon’s direction of travel. Therefore, in studies of phytoplankton biology, the relevant measure of the light field is the photosynthetic available radiation, PAR, defined by

$$\begin{aligned} \text{PAR}(z) &\equiv \int_{350 \text{ nm}}^{700 \text{ nm}} \frac{\lambda}{hc} E_o(z, \lambda) d\lambda \\ &[\text{photons s}^{-1} \text{m}^{-2}] \end{aligned} \quad [6]$$

where  $h = 6.6255 \times 10^{-34} \text{ Js}$  is the Planck constant and  $c = 3.0 \times 10^{17} \text{ nm s}^{-1}$  is the speed of light. The factor  $\lambda/hc$  converts the energy units of  $E_o$  (watts) to quantum units (photons per second). Bio-optical literature often states PAR values in units of mol photons  $\text{s}^{-1} \text{m}^{-2}$  or einst  $\text{s}^{-1} \text{m}^{-2}$  (where one einstein is one mole of photons).

## Inherent Optical Properties

Consider a small volume  $\Delta V$  of water, of thickness  $\Delta r$  as illuminated by a collimated beam of monochromatic light of wavelength  $\lambda$  and spectral radiant power  $\Phi_i(\lambda)$  ( $\text{W nm}^{-1}$ ), as schematically illustrated in **Figure 2**. Some part  $\Phi_a(\lambda)$  of the incident power  $\Phi_i(\lambda)$  is absorbed within the volume of water. Some part  $\Phi_s(\psi, \lambda)$  is scattered out of the beam at an angle  $\psi$ , and the remaining power  $\Phi_t(\lambda)$  is transmitted through the volume with no change in direction. Let  $\Phi_s(\lambda)$  be the total power that is scattered into all directions.

The inherent optical properties usually employed in radiative transfer theory are the absorption and scattering coefficients. In the geometry of **Figure 2**, the absorption coefficient  $a(\lambda)$  is defined as the limit of the fraction of the incident power that is absorbed within the volume, as the thickness becomes small:

$$a(\lambda) \equiv \lim_{\Delta r \rightarrow 0} \frac{1}{\Phi_i(\lambda)} \frac{\Phi_a(\lambda)}{\Delta r} \quad [\text{m}^{-1}] \quad [7]$$

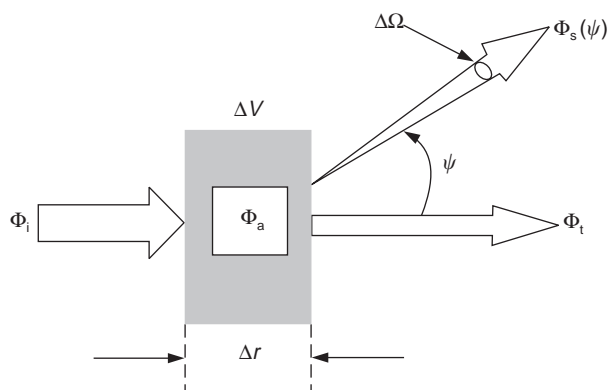


**Figure 2** Geometry used to define inherent optical properties.

The scattering coefficient  $b(\lambda)$  has a corresponding definition using  $\Phi_s(\lambda)$ . The beam attenuation coefficient  $c(\lambda)$  is defined as  $c(\lambda) = a(\lambda) + b(\lambda)$ .

Now take into account the angular distribution of the scattered power, with  $\Phi_s(\psi, \lambda)/\Phi_i(\lambda)$  being the fraction of incident power scattered out of the beam through an angle  $\psi$  into a solid angle  $\Delta\Omega$  centered on  $\psi$ , as shown in **Figure 2**. Then the fraction of scattered power per unit distance and unit solid angle,  $\beta(\psi, \lambda)$ , is

$$\beta(\psi, \lambda) \equiv \lim_{\Delta r \rightarrow 0} \lim_{\Delta\Omega \rightarrow 0} \frac{\Phi_s(\psi, \lambda)}{\Phi_i(\lambda)\Delta r\Delta\Omega} \quad [\text{m}^{-1} \text{sr}^{-1}] \quad [8]$$

The spectral power scattered into the given solid angle  $\Delta\Omega$  is just the spectral radiant intensity scattered into direction  $\psi$  times the solid angle:  $\Phi_s(\psi, \lambda) = I_s(\psi, \lambda)\Delta\Omega$ . Moreover, if the incident power  $\Phi_i(\lambda)$  falls on an area  $\Delta A$ , then the corresponding incident irradiance is  $E_i(\lambda) = \Phi_i(\lambda)/\Delta A$ . Noting that  $\Delta V = \Delta r\Delta A$  is the volume of water that is illuminated by the incident beam gives

$$\beta(\psi, \lambda) = \lim_{\Delta V \rightarrow 0} \frac{I_s(\psi, \lambda)}{E_i(\lambda)\Delta V} \quad [9]$$

This form of  $\beta(\psi, \lambda)$  suggests the name volume scattering function (VSF) and the physical interpretation of scattered intensity per unit incident irradiance per unit volume of water. **Figure 3** shows measured VSFs (at 514 nm) from three greatly different water bodies; the VSF of pure water is shown for comparison. VSFs of sea water typically increase by five or six orders of magnitude in going from  $\psi = 90^\circ$  to  $\psi = 0.1^\circ$  for a given water sample, and scattering at a given angle  $\psi$  can vary by two orders of magnitude among water samples.

Integrating  $\beta(\psi, \lambda)$  over all directions (solid angles) gives the total scattered power per unit incident irradiance and unit volume of water, in other words the spectral scattering coefficient:

$$b(\lambda) = \int_{4\pi} \beta(\psi, \lambda) d\Omega = 2\pi \int_0^\pi \beta(\psi, \lambda) \sin\psi d\psi \quad [10]$$

Eqn. [10] follows because scattering in natural waters is azimuthally symmetric about the incident direction (for unpolarized light sources and randomly oriented scatterers). This integration is often divided into forward scattering,  $0 \leq \psi \leq \pi/2$ , and backward scattering,  $\pi/2 \leq \psi \leq \pi$ , parts. Thus the backscatter coefficient is

$$b_b(\lambda) \equiv 2\pi \int_{\pi/2}^\pi \beta(\psi, \lambda) \sin\psi d\psi \quad [11]$$

The VSFs of **Figure 3** have  $b$  values ranging from  $0.037$  to  $1.824 \text{ m}^{-1}$  and backscatter fractions  $b_b/b$  of  $0.013$  to  $0.044$ .

The preceding discussion assumed that no inelastic-scattering processes are present. However, inelastic scattering does occur owing to fluorescence by dissolved matter or chlorophyll, and to Raman scattering by the water molecules themselves. Power lost from wavelength  $\lambda$  by scattering into wavelength  $\lambda' \neq \lambda$  appears as an increase in the absorption  $a(\lambda)$ . The gain in power at  $\lambda'$  appears as a source term in the radiative transfer equation.

Two more inherent optical properties are commonly used in optical oceanography. The single-scattering albedo is  $\omega_o(\lambda) = b(\lambda)/c(\lambda)$ . The

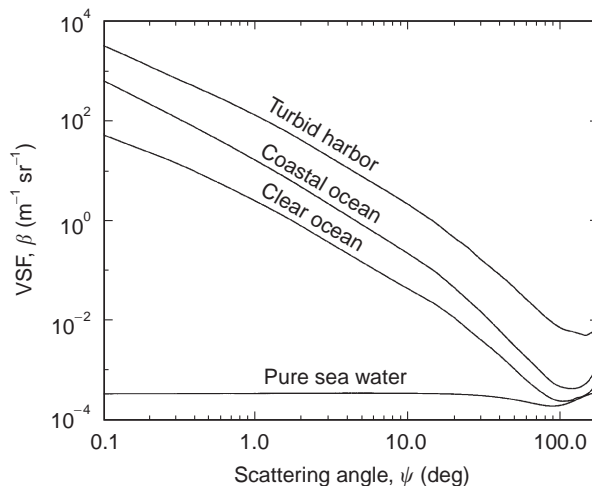


**Figure 3** Volume scattering functions (VSF) measured in three different oceanic waters. The VSF of pure sea water is shown for comparison.

single-scattering albedo is the probability that a photon will be scattered (rather than absorbed) in any given interaction, hence  $\omega_o(\lambda)$  is also known as the probability of photon survival. The volume scattering phase function,  $\tilde{\beta}(\psi, \lambda)$  is defined by

$$\tilde{\beta}(\psi, \lambda) \equiv \frac{\beta(\psi, \lambda)}{b(\lambda)} \quad [\text{sr}^{-1}] \quad [12]$$

Writing the volume scattering function  $\beta(\psi, \lambda)$  as the product of the scattering coefficient  $b(\lambda)$  and the phase function  $\tilde{\beta}(\psi, \lambda)$  partitions  $\beta(\psi, \lambda)$  into a factor giving the strength of the scattering,  $b(\lambda)$  with units of  $\text{m}^{-1}$ , and a factor giving the angular distribution of the scattered photons,  $\tilde{\beta}(\psi, \lambda)$  with units of  $\text{sr}^{-1}$ . A striking feature of the sea water VSFs of Figure 3 is that their phase functions are all similar in shape, with the main differences being in the detailed shape of the functions in the backscatter directions ( $\psi > 90^\circ$ ).

The IOPs are additive. This means, for example, that the total absorption coefficient of a water body is the sum of the absorption coefficients of water, phytoplankton, dissolved substances, mineral particles, etc. This additivity allows the development of separate models for the absorption and scattering properties of the various constituents of sea water.

## The Radiative Transfer Equation

The equation that connects the IOPs and the radiance is called the radiative transfer equation (RTE). Even in the simplest situation of horizontally homogeneous water and time independence, the RTE is a formidable integro-differential equation:

$$\begin{aligned} \cos \theta \frac{dL(z, \theta, \varphi, \lambda)}{dz} = & -c(z, \lambda)L(z, \theta, \varphi, \lambda) \\ & + \int_{4\pi} L(z, \theta', \varphi', \lambda) \\ & \times \beta(z; \theta', \varphi' \rightarrow \theta, \varphi; \lambda) d\Omega' \\ & + S(z, \theta, \varphi, \lambda) \end{aligned} \quad [13]$$

The scattering angle  $\psi$  in the VSF is the angle between the incident direction ( $\theta', \varphi'$ ) and the scattered direction ( $\theta, \varphi$ ). The source term  $S(z, \theta, \varphi, \lambda)$  can describe either an internal light source such as bioluminescence, or inelastically scattered light from other wavelengths. The physical environment of a water body – waves on its surface, the character of its bottom, the incident radiance from the sky – enters the theory via the boundary conditions necessary to solve the RTE. Given the IOPs and suitable boundary conditions, the RTE can be

solved numerically for the radiance distribution  $L(z, \theta, \varphi, \lambda)$ . Unfortunately, there are no shortcuts to computing other radiometric quantities. For example, it is not possible to write down an equation that can be solved directly for the irradiance  $E_d$ ; one must first solve the RTE for the radiance and then compute  $E_d$  by integrating the radiance over direction.

## Apparent Optical Properties

Apparent optical properties are always a ratio of two radiometric variables. This ratioing removes effects of the magnitude of the incident sky radiance onto the sea surface. For example, if the sun goes behind a cloud, the downwelling and upwelling irradiances within the water can change by an order of magnitude within a few seconds, but their ratio will be almost unchanged. (There will still be some change because the directional structure of the underwater radiance will change when the sun's direct beam is removed from the radiance incident onto the sea surface.)

The ratio just mentioned,

$$R(z, \lambda) \equiv \frac{E_u(z, \lambda)}{E_d(z, \lambda)} \quad [14]$$

is called the irradiance reflectance (or irradiance ratio). The remote-sensing reflectance  $R_{rs}(\theta, \varphi, \lambda)$  is defined as

$$R_{rs}(\theta, \varphi, \lambda) \equiv \frac{L_w(\theta, \varphi, \lambda)}{E_d(\lambda)} \quad [\text{sr}^{-1}] \quad [15]$$

where  $L_w$  is the water-leaving radiance, i.e., the total upward radiance minus the sky and solar radiance that was reflected upward by the sea surface.  $L_w$  and  $E_d$  are evaluated just above the sea surface. Both  $R_{rs}(\theta, \varphi, \lambda)$  and  $R(z, \lambda)$  just beneath the sea surface are of great importance in remote sensing, and both can be regarded as a measure of 'ocean color.'  $R$  and  $R_{rs}$  are proportional (to a first-order approximation) to  $b_b/(a + b_b)$ , and measurements of  $R_{rs}$  above the surface or of  $R$  within the water can be used to estimate water quality parameters such as the chlorophyll concentration.

Under typical oceanic conditions, for which the incident lighting is provided by the sun and sky, the radiance and various irradiances all decrease approximately exponentially with depth, at least when far enough below the surface (and far enough above the bottom, in shallow water) to be free of boundary effects. It is therefore convenient to write the

depth dependence of, say,  $E_d(z, \lambda)$  as

$$E_d(z, \lambda) \equiv E_d(0, \lambda) \exp \left[ - \int_0^z K_d(z', \lambda) dz' \right] \quad [16]$$

where  $K_d(z, \lambda)$  is the spectral diffuse attenuation coefficient for spectral downwelling plane irradiance. Solving for  $K_d(z, \lambda)$  gives

$$\begin{aligned} K_d(z, \lambda) &= - \frac{d \ln E_d(z, \lambda)}{dz} \\ &= - \frac{1}{E_d(z, \lambda)} \frac{dE_d(z, \lambda)}{dz} \quad [\text{m}^{-1}] \quad [17] \end{aligned}$$

The beam attenuation coefficient  $c(\lambda)$  is defined in terms of the radiant power lost from a collimated beam of photons. The diffuse attenuation coefficient  $K_d(z, \lambda)$  is defined in terms of the decrease with depth of the ambient downwelling irradiance  $E_d(z, \lambda)$ , which comprises photons heading in all downward directions (a diffuse, or uncollimated, light field).  $K_d(z, \lambda)$  clearly depends on the directional structure of the ambient light field, hence its classification as an apparent optical property. Other diffuse attenuation coefficients, e.g.,  $K_u$ ,  $K_{od}$ , or  $K_{PAR}$ , are defined in an analogous manner, using the corresponding radiometric quantities. In most waters, these  $K$  functions are strongly correlated with the absorption coefficient  $a$  and therefore can serve as convenient, if imperfect, descriptors of a water body. However, AOPs are not additive, which complicates their interpretation in terms of water constituents.

## Optical Constituents of Seawater

Oceanic waters are a witch's brew of dissolved and particulate matter whose concentrations and optical properties vary by many orders of magnitude, so that ocean waters vary in color from the deep blue of the open ocean, where sunlight can penetrate to depths of several hundred meters, to yellowish-brown in a turbid estuary, where sunlight may penetrate less than a meter. The most important optical constituents of sea water can be briefly described as follows.

### Sea Water

Water itself is highly absorbing at wavelengths below 250 nm and above 700 nm, which limits the wavelength range of interest in optical oceanography to the near-ultraviolet to the near infrared.

### Dissolved Organic Compounds

These compounds are produced during the decay of plant matter. In sufficient concentrations these compounds can color the water yellowish brown; they are therefore generally called yellow matter or colored dissolved organic matter (CDOM). CDOM absorbs very little in the red, but absorption increases rapidly with decreasing wavelength, and CDOM can be the dominant absorber at the blue end of the spectrum, especially in coastal waters influenced by river runoff.

### Organic Particles

Biogenic particles occur in many forms.

**Bacteria** Living bacteria in the size range 0.2–1.0  $\mu\text{m}$  can be significant scatterers and absorbers of light, especially at blue wavelengths and in clean oceanic waters, where the larger phytoplankton are relatively scarce.

**Phytoplankton** These ubiquitous microscopic plants occur with incredible diversity of species, size (from less than 1  $\mu\text{m}$  to more than 200  $\mu\text{m}$ ), shape, and concentration. Phytoplankton are responsible for determining the optical properties of most oceanic waters. Their chlorophyll and related pigments strongly absorb light in the blue and red and thus, when concentrations are high, determine the spectral absorption of sea water. Phytoplankton are generally much larger than the wavelength of visible light and can scatter light strongly.

**Detritus** Nonliving organic particles of various sizes are produced, for example, when phytoplankton die and their cells break apart, and when zooplankton graze on phytoplankton and leave cell fragments and fecal pellets. Detritus can be rapidly photooxidized and lose the characteristic absorption spectrum of living phytoplankton, leaving significant absorption only at blue wavelengths. However, detritus can contribute significantly to scattering, especially in the open ocean.

### Inorganic Particles

Particles created by weathering of terrestrial rocks can enter the water as wind-blown dust settles on the sea surface, as rivers carry eroded soil to the sea, or as currents resuspend bottom sediments. Such particles range in size from less than 0.1  $\mu\text{m}$  to tens of micrometers and can dominate water optical properties when present in sufficient concentrations.

Particulate matter is usually the major determinant of the absorption and scattering properties

of sea water and is responsible for most of the temporal and spatial variability in these optical properties. A central goal of research in optical oceanography is to understand how the absorption and scattering properties of these various constituents relate to the particle type (e.g., microbial species or mineral composition), present conditions (e.g., the physiological state of a living microbe, which in turn depends on nutrient supply and ambient lighting), and history (e.g., photo-oxidation of pigments in dead cells). Bio-geo-optical models have been developed that attempt (with varying degrees of success) to predict the IOPs in terms of the chlorophyll concentration or other simplified measures of the composition of a water body.

### Examples of Underwater Light Fields

Solving the radiative transfer equation requires mathematically sophisticated and computationally intensive numerical methods. *HydroLight* is a widely used software package for numerical solution of oceanographic radiative transfer problems. The input to *HydroLight* consists of the absorption and scattering coefficients of each constituent of the water body (microbial particles, dissolved substances, mineral particles, etc.) as functions of depth and wavelength, the corresponding scattering phase functions, the sea state, the sky radiance incident onto the sea surface, and the reflectance properties of the bottom boundary (if the water is not assumed infinitely deep). *HydroLight* solves the one-dimensional, time-independent radiative transfer equation, including inelastic scattering effects, to obtain the radiance distribution  $L(z, \theta, \varphi, \lambda)$ . Other quantities of interest such as irradiances or reflectances are then computed using their definitions and the solution radiance distribution.

To illustrate the range of behavior of underwater light fields, *HydroLight* was run for two greatly different water bodies. The first simulation used a chlorophyll profile measured in the Atlantic Ocean north of the Azores in winter. The water was well mixed to a depth of over 100 m. The chlorophyll concentration  $Chl$  varied between 0.2 and 0.3 mg m<sup>-3</sup> between the surface and 116 m depth; it then dropped to less than 0.05 mg m<sup>-3</sup> below 150 m depth. The water was oligotrophic, case 1 water, and commonly used bio-optical models for case 1 water were used to convert the chlorophyll concentration to absorption and scattering coefficients (which were not measured). A scattering phase function similar in shape to those seen in **Figure 3** was used for the particles; this phase function had a backscatter fraction of  $b_b/b = 0.018$ . The second

simulation was for an idealized, case 2 coastal water body containing 5 mg m<sup>-3</sup> of chlorophyll and 2 g m<sup>-3</sup> of brown-colored mineral particles representing resuspended sediments. Bio-optical models and measured mass-specific absorption and scattering coefficients were used to convert the chlorophyll and mineral concentrations to absorption and scattering coefficients. The large microbial particles of low index of refraction were assumed to have a phase function with  $b_b/b = 0.005$ , and the small mineral particles of high index of refraction had  $b_b/b = 0.03$ . The water was assumed to be well mixed and to have a brown mud bottom at a depth of 10 m. Both simulations used a clear sky radiance distribution appropriate for midday in January at the Azores location. The sea surface was covered by capillary waves corresponding to a 5 m s<sup>-1</sup> wind speed.

**Figure 4** shows the component and total absorption coefficients just beneath the sea surface for these two hypothetical water bodies, and **Figure 5** shows the corresponding scattering coefficients. For the case 1 water, the total absorption is dominated by chlorophyll at blue wavelengths and by the water itself at wavelengths greater than 500 nm. However, the water makes only a small contribution to the total scattering. In the case 2 water, absorption by the mineral particles is comparable to or greater than that by the chlorophyll-bearing particles, and water dominates only in the red. The mineral particles are the primary scatterers.

**Figures 6** and **7** show the radiance in the azimuthal plane of the sun as a function of polar viewing direction and wavelength, for selected depths. For the case 1 simulation (**Figure 6**), the depths shown are zero, just beneath the sea surface, and 100 m; for the case 2 simulation (**Figure 7**), the depths are zero and 10 m, which is at the bottom. Note that the radiance axis is logarithmic. A viewing direction of  $\theta_v = 0$  corresponds to looking straight down and seeing the upwelling radiance (photons traveling straight up). Near the sea surface, the angular dependence of the radiance distribution is complicated because of boundary effects such as internal reflection (the bumps near  $\theta_v = 90^\circ$ , which is radiance traveling horizontally) and refraction of the sun's direct beam (the large spike near  $\theta_v = 140^\circ$ ). As the depth increases, the angular shape of the radiance distribution smooths out as a result of multiple scattering. By 100 m in the case 1 simulation, the shape of the radiance distribution is approaching its asymptotic shape, which is determined only by the IOPs. In the case 2 simulation, the upwelling radiance ( $-90^\circ \leq \theta_v \leq 90^\circ$ ) at the bottom is isotropic; this is a consequence of having

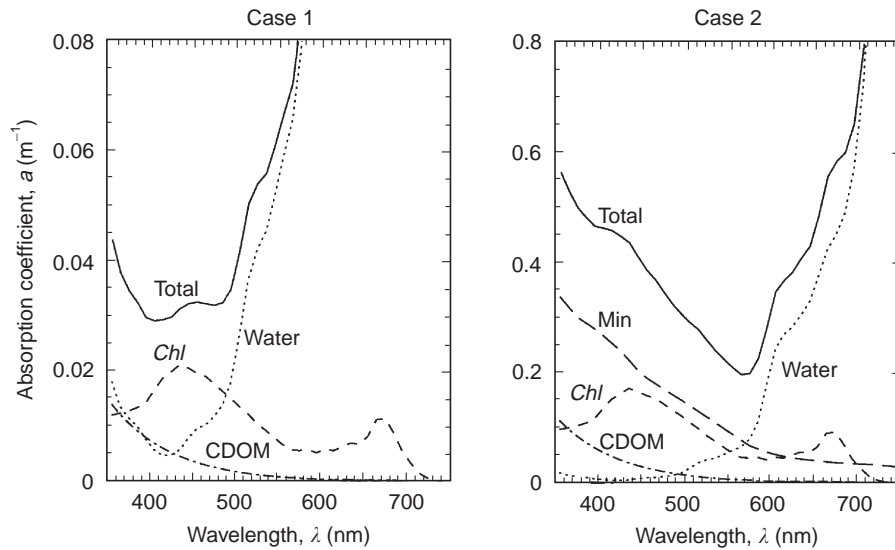


**Figure 4** Absorption coefficients for the case 1 and case 2 water bodies. The contributions by the various components are labeled.

assumed the mud bottom to be a Lambertian reflecting surface. As the depth increases, the color of the radiance becomes blue for the case 1 water and greenish-yellow for the case 2 water. In the case 1 simulation at 100 m, there is a prominent peak in the radiance near 685 nm, even though the solar radiance has been filtered out by the strong absorption by water at red wavelengths. This peak is due to chlorophyll fluorescence, which is transferring energy from blue to red wavelengths, where it is emitted isotropically.

As already noted, the extensive information contained in the full radiance distribution is seldom

needed. A biologist would probably be interested only in the scalar irradiance  $E_o$ , which is shown at selected depths in **Figure 8**. This irradiance was computed by integrating the radiance over all directions. Although the irradiances near the surface are almost identical, the decay of these irradiances with depth is much different in the case 1 and case 2 waters.

The remote-sensing reflectance  $R_{rs}$ , the quantity of interest for ‘ocean color’ remote sensing, is shown in **Figure 9** for the two water bodies. The shaded bars at the bottom of the figure show the nominal SeaWiFS sensor bands. The SeaWiFS

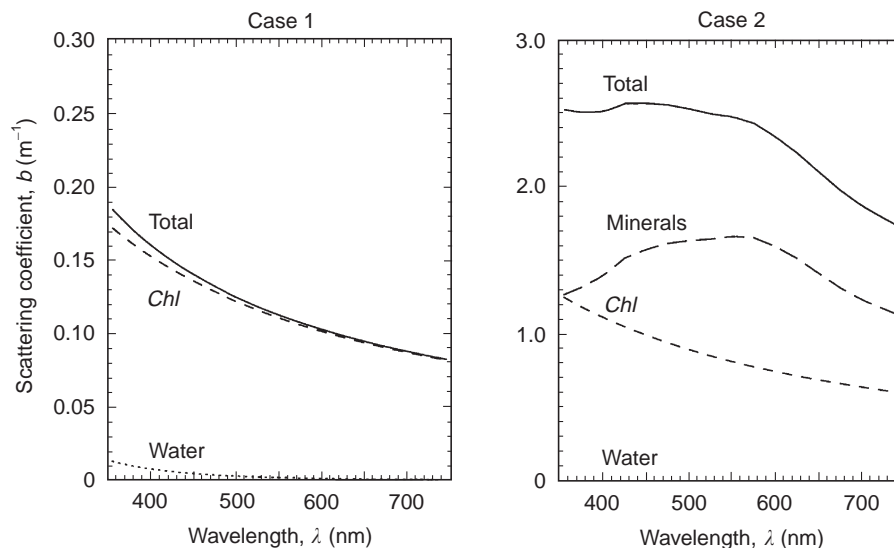


**Figure 5** Scattering coefficients for the case 1 and case 2 water bodies. The contributions by the various components are labeled (CDOM is nonscattering).



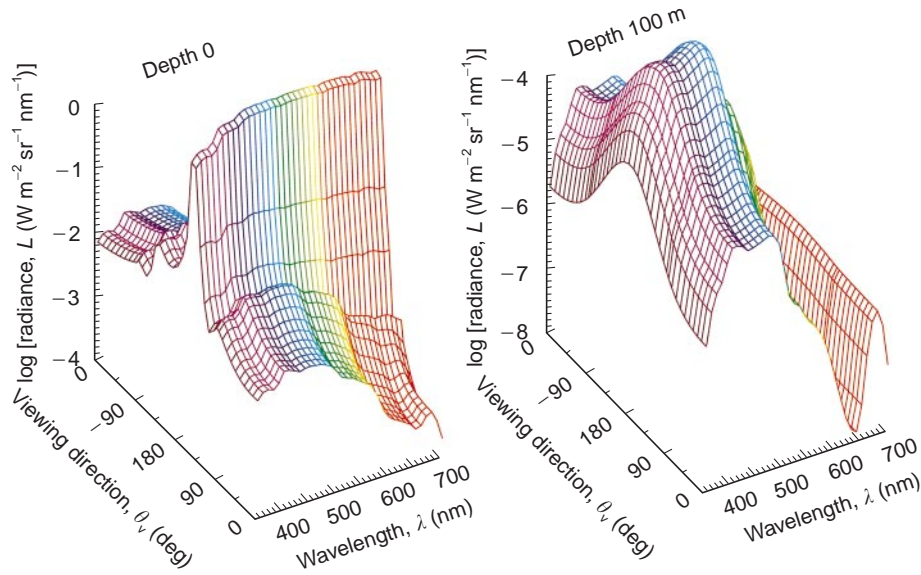


**Figure 6** The case 1 water radiance distribution in the azimuthal plane of the sun at depth 0 (just below the sea surface) and at 100 m.

algorithm for retrieval of the chlorophyll concentration uses a function of the ratio  $R_{rs}(490\text{ nm})/R_{rs}(555\text{ nm})$ . When applied to these  $R_{rs}$  spectra, the SeaWiFS algorithm retrieves a value of  $Chl = 0.24\text{ mg m}^{-3}$  for the case 1 water, which is close to the average value of the measured profile over the upper few tens of meters of the water column. However, when applied to the case 2 spec-

trum, the SeaWiFS algorithm gives  $Chl = 8.88\text{ mg m}^{-3}$ , which is almost twice the value of  $5.0\text{ mg m}^{-3}$  used in the simulation. This error results from the presence of the mineral particles, which are not accounted for in the SeaWiFS chlorophyll retrieval algorithm.

These *Hydrolight* simulations highlight the fact that it is now possible to compute accurate underwater

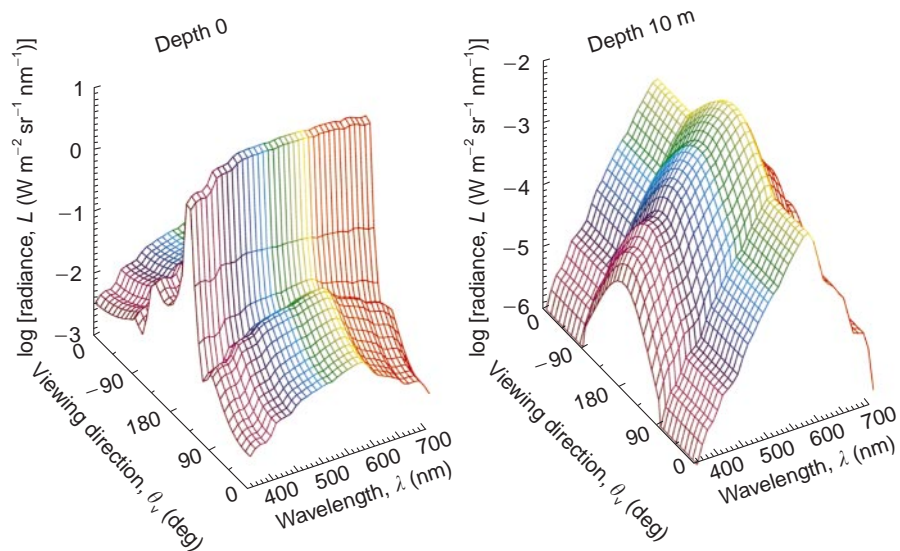


**Figure 7** The case 2 water radiance distribution in the azimuthal plane of the sun at depth 0 (just below the sea surface) and at 10 m.

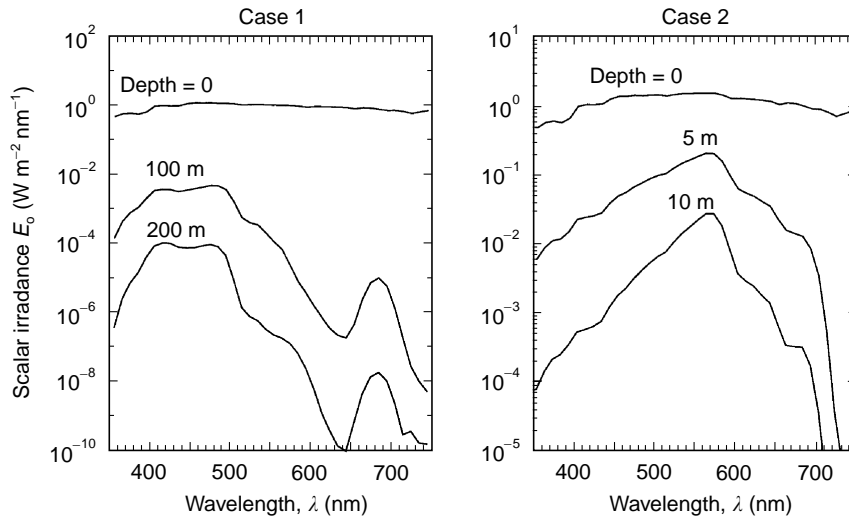


**Figure 8** The scalar irradiance  $E_0$  at selected depths for the case 1 and case 2 waters.

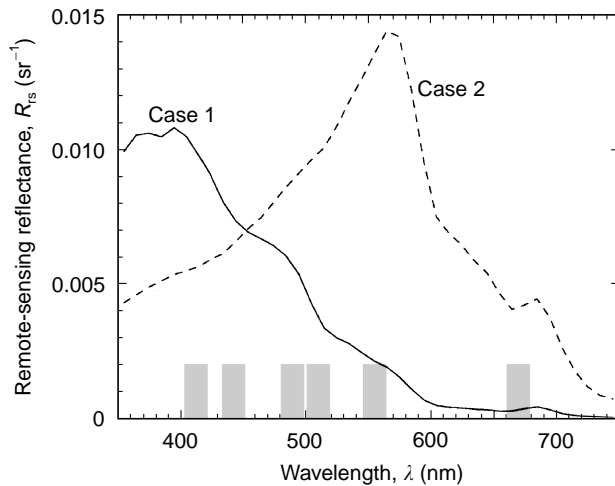


**Figure 9** The remote-sensing reflectance  $R_{rs}$  for the case 1 and case 2 waters.

radiance distributions given the IOPs and boundary conditions. The difficult science lies in learning how to predict the IOPs for the incredible variety of water constituents and environmental conditions found in the world's oceans, and in learning how to interpret measurements such as  $R_{rs}$ . The development of bio-geo-optical models for case 2 waters, in particular, is a research topic for the next decades.

## See also

**Bacterioplankton. Bio-optical Models. IR Radiometers. Ocean Color from Satellites.**

## Further Reading

- Bukata RP, Jerome JH, Kondratyev KY and Pozdnyakov DV (1995) *Optical Properties and Remote Sensing of Inland and Coastal Waters*. New York: CRC Press.
- Caimi FM (ed.) (1995) *Selected Papers on Underwater Optics*. SPIE Milestone Series, vol. MS 118. Bellingham, WA: SPIE Optical Engineering Press.
- Jerlov NG (1976) *Marine Optics*. Amsterdam: Elsevier.
- Kirk JTO (1994) *Light and Photosynthesis in Aquatic Ecosystems*, 2nd edn. New York: Cambridge University Press.
- Mobley CD (1994) *Light and Water: Radiative Transfer in Natural Waters*. San Diego: Academic Press.
- Mobley CD (1995) The optical properties of water. In Bass M (ed.) *Handbook of Optics*, 2nd edn, vol. I. New York: McGraw Hill.
- Mobley CD and Sundman LK (2000) *Hydrolight 4.1 Users' Guide*. Redmond, WA: Sequoia Scientific. [See also [www.sequoiasci.com/hydrolight.html](http://www.sequoiasci.com/hydrolight.html)]
- Shifrin KS (1988) *Physical Optics of Ocean Water*. AIP Translation Series. New York: American Institute of Physics.
- Spinrad RW, Carder KL and Perry MJ (1994) *Ocean Optics*. New York: Oxford University Press.
- Walker RE (1994) *Marine Light Field Statistics*. New York: Wiley.